



HAL
open science

Feedback Classification and Optimal Control with Applications to the Controlled Lotka-Volterra Model

Bernard Bonnard, Jérémy Rouot

► **To cite this version:**

Bernard Bonnard, Jérémy Rouot. Feedback Classification and Optimal Control with Applications to the Controlled Lotka-Volterra Model. 2024. hal-03917363v2

HAL Id: hal-03917363

<https://inria.hal.science/hal-03917363v2>

Preprint submitted on 24 May 2024 (v2), last revised 13 Aug 2024 (v3)

HAL is a multi-disciplinary open access archive for the deposit and dissemination of scientific research documents, whether they are published or not. The documents may come from teaching and research institutions in France or abroad, or from public or private research centers.

L'archive ouverte pluridisciplinaire **HAL**, est destinée au dépôt et à la diffusion de documents scientifiques de niveau recherche, publiés ou non, émanant des établissements d'enseignement et de recherche français ou étrangers, des laboratoires publics ou privés.



Distributed under a Creative Commons Attribution 4.0 International License

2 **Feedback Classification and Optimal Control with Applications to the**
3 **Controlled Lotka–Volterra Model**

4 Bernard Bonnard^a and Jérémy Rouot^b

5 ^aInstitut Mathématique de Bourgogne and Inria Sophia Antipolis, 9 rue Alain Savary, 21 000 Dijon

6 ^bUniv Brest, UMR CNRS 6205, Laboratoire de Mathématiques de Bretagne Atlantique, Brest

7

8 **ARTICLE HISTORY**

9 Compiled May 23, 2024

10 *Dedicated to Roger W. Brockett and Ivan Kupka.*

11 **ABSTRACT**

12 Let M be a σ -compact C^∞ manifold of dimension $n \geq 2$ and consider a single-input control system: $\dot{x}(t) = X(x(t)) + u(t)Y(x(t))$, where X, Y are C^∞ vector fields on M . We prove
13 that there exist an open set of pairs (X, Y) for the C^∞ -Whitney topology such that they
14 admit singular abnormal rays so that the spectrum of the projective singular Hamiltonian
15 dynamics is feedback invariant. It is applied to controlled Lotka–Volterra dynamics where
16 such rays are related to shifted equilibria of the free dynamics.
17

18 **KEYWORDS**

19 Feedback classification; Nonlinear systems; Lotka–Volterra model; Optimal control; Direct
20 numerical methods

21 **1. Introduction**

22 Consider a single-input affine control system on a σ -compact C^∞ manifold of dimension
23 $n \geq 2$ defined by

$$\frac{dx}{dt}(t) = X(x(t)) + u(t)Y(x(t)), \quad (1)$$

24 where X, Y are C^∞ vector fields on M and the set of admissible controls \mathcal{U} is the set of
25 bounded measurable mappings $u : [0, T(u)] \mapsto \mathbb{R}$, $T(u) > 0$.

26 Let (X, Y) and (X', Y') be two such pairs. They are called *feedback equivalent* if there
27 exist a C^∞ diffeomorphism φ on M and a feedback $u = \alpha(x) + \beta(x)u'$, where α, β are C^∞
28 mappings and β invertible so that

29 (i) $X' = \varphi * X + (\varphi * Y) \cdot \alpha$,

30 (ii) $Y' = (\varphi * Y) \cdot \beta$,

31 where if Z is a C^∞ vector field $\varphi * Z$ is the image of Z by φ given in local coordinates by

$$\varphi * Z = \left(\frac{\partial \varphi}{\partial x} \right)^{-1} (Z \circ \varphi).$$

32 This action defines a group structure G_f on the set of triplets $\{g = (\varphi, \alpha, \beta)\}$ called the *feed-*
33 *back group*.

34 It is well known from geometric linear system theory [23] that, restricting to linear au-
35 tonomous controllable systems: $\dot{x}(t) = Ax(t) + u(t)b$, A being a constant matrix and b a
36 constant vector, every such pairs (A, b) and (A', b') are feedback equivalent, restricting to
37 linear diffeomorphisms and feedbacks: $u = \alpha \cdot x + \beta u'$, $\beta \neq 0$ constant.

38 The feedback equivalence for control affine systems was studied in the earliest refer-
39 ence [4] (see also [1]) in relation with the time–minimal geodesics corresponding to the so-
40 called *singular trajectories*. More precisely consider the pair (X, Y) and denote by $x(\cdot, x_0, u)$
41 the response to $u(\cdot) \in \mathcal{U}$ starting at time $t = 0$ from x_0 . Fixing t_f , the *fixed extremity map-*
42 *ping* at time t_f is the map $E^{x_0, t_f} : \mathcal{U} \ni u \mapsto x(t_f, x_0, u) \in M$. If t_f is free, the extremity map-
43 ping is the map $E^{x_0} : \mathcal{U} \ni u \mapsto x(\cdot, x_0, u)$. If we endow the set of controls with the L^∞ -norm
44 topology both maps are Fréchet differentiable and they have singularities, that is the im-
45 age of L^∞ by the derivative is not of full rank n . Such a pair $(x(\cdot), u(\cdot))$ is called *singular*
46 for the fixed time case and if the final time is not fixed such singular trajectories are called
47 exceptional or *abnormal*.

48 Singular trajectories can be parametrized thanks to the Maximum Principle [16] as pro-
49 jection of *singular extremal* pairs $(z(\cdot), u(\cdot))$, $z = (x, p)$ where p is non vanishing adjoint
50 vector solutions of the Hamiltonian dynamics:

$$\begin{aligned} \frac{dz}{dt}(t) &= H_X(z(t)) + u(t) H_Y(z(t)), \\ H_Y(z(t)) &= 0, \end{aligned} \tag{2}$$

51 where $H_X = p \cdot X(x)$ and $H_Y = p \cdot Y(x)$ are respectively the Hamiltonian lifts of X, Y , $H_X +$
52 uH_Y is the pseudo Hamiltonian and additionally in the abnormal case, we have:

$$H_X(z(t)) = 0.$$

53 Given a pair (X, Y) the *collinearity set* is the set \mathcal{C} of points $x \in M$ such that $X(x)$ and
54 $Y(x)$ are linearly dependent. Clearly it is a feedback invariant. Taking a point x_e in \mathcal{C} there
55 exist a *constant* u_e so that $X(x_e) + u_e Y(x_e) = 0$ and the pair (x_e, u_e) is called a forced equili-
56 brium.

57 The contribution of this article is to construct if $n \geq 2$ a set of pairs (X, Y) of codimension
58 n in the jets space such that there exist abnormal trajectories reduced to isolated point x_0 ,
59 which can be lifted into lines ℓ in the projective space $PT_{x_0}^* M$ called *abnormal rays* and
60 the whole spectrum of the *projectivized* linearized dynamics defined by (2) is feedback
61 invariant.

62 This result can be illustrated by the following $2d$ -case, $x = (x_1, x_2)$,

$$\begin{aligned} \dot{x}_1 &= \lambda x_1 + x_2^2 \\ \dot{x}_2 &= u \end{aligned} \tag{3}$$

63 in which the singular line is the axis $x_2 = 0$ on which the singular dynamics is given by
64 $\dot{x}_1 = \lambda x_1$ and the abnormal point is the equilibrium point 0. Denoting $p = (p_1, p_2)$ the

65 adjoint vector one has $p_2 = 0$ since $H_Y = 0$ and the adjoint vector is given by $\dot{p}_1 = -\lambda p_1$.
 66 Hence the ray at $T_0^* \mathbb{R}^2$ is $\ell : p_1(t) = e^{-\lambda t} p_1(0)$. The singular Hamiltonian dynamics reads

$$\dot{x}_1 = \lambda x_1, \quad \dot{p}_1 = -\lambda p_1.$$

67 Clearly λ is feedback invariant and the projectivized dynamics is given by the dynamics of
 68 $v = x_1 / p_1$ with singular point at $v = 0$ with eigenvalue 2λ (the projectivized invariant).

69 Note that in the n -dimensional case, for each ray one gets $2n - 3$ eigenvalues to classify
 70 the systems.

71 This result is applied to analyze vermin reduction for controlled *Lotka–Volterra* dyna-
 72 mics in the cone $M = \mathbb{R}_{\geq 0}^n$ where the equations read

$$\frac{dx}{dt}(t) = (\text{diag}x(t)) (Ax(t) + r + u(t)\mathbf{C}) \quad (4)$$

73 with $x := (x_1, \dots, x_n)^\top$ is the vector of interacting species, $\text{diag}x$ denotes in short the diago-
 74 nal matrix with diagonal coefficients x_i , $A = (a_{ij})$ is the matrix of interaction coefficients
 75 and $r = (r_1, \dots, r_n)^\top$ is the individual growth vector without interaction. The constant vector
 76 $\mathbf{C} = (\epsilon_1, \dots, \epsilon_n)^\top$ describes the effect of probiotic or antibiotic agents to reduce the popula-
 77 tion of the infecting agent, which can be taken as the x_1 -population. The optimal control
 78 problem is a *Mayer problem*: $\min_{u(\cdot)} x_1(t_f)$, which can be formulated in the dual form as:
 79 $\min_{u(\cdot)} t_f$, $x_1(t_f) = d$, where d is a desired amount of population x_1 at final time t_f , taken
 80 as a parameter. More generally we shall consider any Mayer problem: $\min_{u(\cdot)} \phi(x(t_f))$ with
 81 ϕ is a smooth mapping from M to \mathbb{R} .

82 The free motion was studied by the historical contributors Lotka and Volterra, genera-
 83 lizing the prey–predator model for populations dynamics [21]. The interest of the model is
 84 to get easily computable equilibria using linear analysis only. In the regular case where A
 85 is invertible, the *interior equilibrium* is $x_e := -A^{-1}r$ and the dynamics is related in parti-
 86 cular to interaction of x_e with the trivial boundary equilibrium 0. A large amount of liter-
 87 ature was devoted to analyze the dynamics in the $2d$ or $3d$ case starting from the seminal
 88 complete analysis in the prey–predator model. In particular in the case of competitive sys-
 89 tems, the achievement in the $3d$ -case was the explicit analysis of the limit set of the origin
 90 to determine the boundary of the basin of repulsion of this point. Related references are
 91 [11, 24, 19] and in particular the May–Leonard model [15] will serve as case study.

92 An important very recent application of controlled Lotka–Volterra model comes from
 93 the control of complex microbiota, see the work by Jones et al [12] based on the Stein et
 94 al study [20] to model the *C. difficile* infection of the intestinal microbiote. It contains 11
 95 interaction species and can admit up to 2^{11} equilibria. Hence the analysis is a huge task.
 96 More modestly we shall concentrate our computation to specific $2d$ and $3d$ models to il-
 97 lustrate our techniques. Besides the biological applications, the controlled Lotka–Volterra
 98 model allows algebraic computations of the forced equilibria, which are by construction
 99 shifted equilibria of the free equilibria and hence in fine one can compute in this case, the
 100 spectrum of corresponding ray abnormal solutions. We show that this information is rele-
 101 vant in an applicative context to analyze a $3d$ May and Leonard model corresponding to a
 102 certain microbiote with three species using antibiotic and probiotic. Recent contribution
 103 [7] presents a protocol based on a MPC tracking algorithm of a trajectory computed with
 104 a direct method. The first consists in reaching the invariant manifold – carrying simplex
 105 – in minimum time using antibiotic only. The second phase of the treatment focuses on
 106 the asymptotic dynamics in the $2d$ carrying simplex, where the aim is to reach an healthy
 107 region using probiotics only. This article presents an alternative MPC algorithm for the

108 second phase in which we reach an healthy region in minimum time (see also [6, 8]).

109 This article is organized in four sections. In section 2, we make a recap of properties
 110 of singular trajectories and their parametrization, thanks to the Maximum Principle as an
 111 Hamiltonian dynamics in the projectivized cotangent bundle. We introduce the basic con-
 112 cepts of transversality theory in the jets space [14] to formulate in a neat geometric frame-
 113 work the main result of this article concerning feedback invariants. In section 3, we apply
 114 this theorem to classify controlled Lotka–Volterra dynamics in dimension 2 or 3. We point
 115 out some applications to controlled stability and time minimal syntheses. The final sec-
 116 tion 4 relates those calculations based on the Maximum Principle in the permanent case
 117 to the computations of optimal solution of vermin reduction in the sampled–data control
 118 frame.

119 2. A brief recap about singular trajectories and main result

120 This section is based on the results of [4] and [5], which are briefly presented to deduce
 121 the classification result. It combines the techniques from transversality theory in the jets
 122 space, see [14], and elementary geometric invariant theory [10].

123 2.1. Notations and general results

124 Let M be a σ –compact C^∞ (smooth) manifold of dimension $n \geq 2$. We introduce the fol-
 125 lowing notations:

- 126 • TM is the tangent space of M and $T_x M$ is the tangent space at $x \in M$.
- 127 • T^*M is the cotangent space of M and T_x^*M is the cotangent space at $x \in M$. The
 128 null section of T^*M is denoted by 0 and $(T^*M)_0 = T^*M \setminus \{0\}$. We note PT^*M the
 129 projectivized cotangent space i.e. $PT^*M = T^*M/\mathbb{R}^*$ and $[z]$ is the equivalence class
 130 of z in PT^*M .
- 131 • For any integer N , $J^N TM$ is the space of all N –jets of vector fields i.e. Taylor expan-
 132 sions up to order N and $JTM = \cup_{N \geq 0} J^N TM$ is the jets space.
- 133 • $VF(M)$ is the vector space of all smooth vector fields on M endowed with the Whit-
 134 ney topology.
- 135 • We denote by $z = (x, p)$ the canonical coordinates on (T^*M, ω) , where ω is the Dar-
 136 boux form induced by the Liouville form.
- 137 • Take $(X, Y) \in VF(M)$, the Lie bracket is calculated in local coordinates with the con-
 138 vention:

$$[X, Y](x) := \frac{\partial X}{\partial x}(x)Y(x) - \frac{\partial Y}{\partial x}(x)X(x).$$

- 139 • Given any smooth function H defined on an open subset Ω of T^*M , \vec{H} denotes the
 140 Hamiltonian vector field defined by H on Ω , $\vec{H} := (\partial_p H, -\partial_x H)$. Given H_1, H_2 on M ,
 141 $\{H_1, H_2\}$ denotes the Poisson bracket:

$$\{H_1, H_2\}(z) := dH_1(\vec{H}_2(z)) = \omega(H_1, H_2).$$

- 142 • If $X \in VF(M)$, H_X denotes the Hamiltonian lift: $H_X(x) := p \cdot X(x)$. Given $(X, Y) \in$
 143 $VF(M)$, one has $\{H_X, H_Y\} = H_{[X, Y]}$.

- 144 • Finally, to each pair (X, Y) of vector fields on M , we associate the single-input con-
145 trol affine system:

$$\frac{dx}{dt}(t) = X(x(t)) + u(t)Y(x(t)), \quad u(t) \in \mathbb{R}, \quad x \in M. \quad (5)$$

146 The study of time-minimal trajectory of (5) leads to introduce the *extremal trajectories*:
147 $(z, u) : [0, T] \rightarrow T^*M \times \mathbb{R}$, $T > 0$, such that

- 148 (1) z is absolutely continuous, u is measurable and bounded,
149 (2) $z(t) \neq 0$ (0 being the null section) for all $t \in [0, T]$,
150 (3) $\frac{dz}{dt}(t) = \vec{H}_X(z(t)) + u(t)\vec{H}_Y(z(t))$ for a.e. $t \in [0, T]$,
151 (4) $\vec{H}_X(z(t)) + u(t)H_Y(z(t)) = \max_{v \in \mathbb{R}} H_X(z(t)) + vH_Y(z(t))$ for a.e. $t \in [0, T]$ or equiva-
152 lently

$$H_Y(z(t)) = 0, \quad \text{for all } t \in [0, T] \quad (6)$$

153 since $z \mapsto H_Y(z)$ is continuous.

154 **Definition 2.1.** A curve $(z, u) : [0, T] \rightarrow T^*M \times \mathbb{R}$ satisfying the above conditions (1)–(4) is
155 called a singular extremal and its projection $(\Pi_M(z, u), u) = (x, u)$ is a singular trajectory.
156 Denoting $z = (x, p)$, p is then the adjoint (non zero) vector.

157 **Proposition 2.2.** Let $(z, u) = (x, p, u)$ be a singular extremal on $[0, T]$. Then:

- 158 • The Fréchet derivative of the fixed time extremity mapping $E^{x(0), t_f}$ along $(x(\cdot), u(\cdot))$ is
159 given by the linear dynamics:

$$\delta_1 \dot{x}(t) = A(t)\delta_1 x(t) + u(t)b(t) \quad (7)$$

160 with $A = \frac{\partial X}{\partial x}(x(t)) + u(t)\frac{\partial Y}{\partial x}(x(t))$ and $b(t) = Y(x(t))$ with initial condition $\delta_1 x(0) = 0$.

- 161 • The adjoint vector $p(\cdot)$ is orthogonal to the image of the Fréchet derivative called the
162 first order Pontryagin space vector.

163 One can easily calculate with the Maximum Principle many singular trajectories (x, u) .
164 Indeed deriving twice with respect to t the equation (6) we get for a.e. $t \in [0, T]$:

$$\begin{aligned} H_Y(z(t)) &= \{H_Y, H_X\}(z(t)) = 0, \\ \{\{H_Y, H_X\}, H_X\}(z(t)) + u(t)\{\{H_Y, H_X\}, H_Y\}(z(t)) &= 0. \end{aligned} \quad (8)$$

165 **Definition 2.3.** A singular extremal (z, u) on $[0, T]$ is called of minimal order if $\mathcal{R} =$
166 $\{t \in [0, T], \{\{H_X, H_Y\}, H_Y\}(z(t)) \neq 0\}$ is dense in $[0, T]$.

167 **Proposition 2.4.** Let (z, u) be a singular extremal and \mathcal{R} be a non empty set, then:

- 168 • z restricted to \mathcal{R} is smooth,
169 • the set $\Sigma' = \{z, H_Y(z) = \{H_Y, H_X\}(z) = 0\}$ is invariant for the singular dynamics, which
170 is given on Σ' by:

$$\frac{dz}{dt}(t) = \vec{H}_X(z(t)) + u_s(z(t))\vec{H}_Y(z(t)) \quad (9)$$

171 where $u_s(z)$ is the singular dynamics feedback:

$$u_s(z) = \frac{\{\{H_X, H_Y\}, H_X\}(z)}{\{\{H_Y, H_X\}, H_Y\}(z)}. \quad (10)$$

172 **Proposition 2.5.** Let (X, Y) be a pair such that the open subset Ω of all $z \in (T^*M)_0$ such that
 173 $\{z, \{\{H_X, H_Y\}, H_Y\}(z) \neq 0\}$ is not empty. Let $H_s : \Omega \rightarrow \mathbb{R}$ be the true Hamiltonian:

$$H_s := H_X + \frac{\{\{H_X, H_Y\}, H_X\}(z)}{\{\{H_Y, H_X\}, H_Y\}(z)} H_Y \quad (11)$$

174 restricted to the set $\Sigma' : \{z, H_Y(z) = \{H_Y, H_X\}(z) = 0\}$. Then there exist an open set in $VF(M) \times$
 175 $VF(M)$ such that for any couple (X, Y) in this set, Ω is open and dense and the set of all $z \in \Sigma'$
 176 is a codimension 2 symplectic manifold of Ω for the induced symplectic form: $\omega|_{\Sigma'}$.

177 **Notations 2.6.** Restricting to such pairs \mathcal{G} (called good pairs), denote:

- 178 • $\Sigma : \{z, H_Y(z) = 0\}$ the switching surface.
- 179 • \vec{H}_s the Hamiltonian dynamics restricted to $\Sigma' \subset \Sigma$ with $\Sigma' : H_Y(z) = \{H_Y, H_X\}(z) = 0$.
- 180 • Let λ_s be the mapping $\mathcal{G} \ni (X, Y) \mapsto (\vec{H}_s, \Sigma)$.

181 2.2. Action of the feedback group G_f on the set of good pairs

182 We shall briefly recall the results of [4]. First of all, borrowed from elementary geometric
 183 invariant theory [10], we have.

184 **Definition 2.7.** Let E, F be two \mathbb{R} -vector spaces and let G be a group acting linearly on E
 185 and F . An homomorphism $\mathfrak{X} : G \rightarrow \mathbb{R}^*$ is called a character. Let \mathfrak{X} be a character. A semi-
 186 invariant of weight \mathfrak{X} is a map $\lambda : E \rightarrow \mathbb{R}$ such that $\forall g \in G, \forall x \in E, \lambda(g \cdot x) = \mathfrak{X}(g)\lambda(x)$. It is
 187 called an invariant if $\mathfrak{X} = 1$. A map $\lambda : E \rightarrow F$ is a semi-covariant of weight \mathfrak{X} if $\forall g \in G, \forall x \in$
 188 $E, \lambda(g \cdot x) = \mathfrak{X}(g)g \cdot \lambda(x)$ and λ is called a covariant if $\mathfrak{X} = 1$.

189 The action of $(\varphi, \alpha, \beta) \in G_f$ can be lifted as the action of Matthieu symplectomorphisms
 190 $\vec{\varphi}$ on T^*M defined in canonical coordinates by $x = \varphi(y), p = q \frac{\partial \varphi^{-1}}{\partial y}$. The action of (φ, α, β)
 191 on (\vec{H}_s, Σ) being reduced to the action of φ only. Also note that $\Sigma : H_X(z) = 0$ codes the
 192 distribution: $x \mapsto \text{span}Y(x)$.

193 **Proposition 2.8.** Restricting to good pairs (X, Y) , λ_s is a covariant, that is the following
 194 diagram is commutative:

$$\begin{array}{ccc} \mathcal{G} \ni (X, Y) & \xrightarrow{\lambda_s} & \lambda_s(X, Y) \\ G_f \downarrow & \circlearrowleft & \downarrow G_f \\ \mathcal{G} \ni (X', Y') & \xrightarrow{\lambda_s} & \lambda_s(X', Y') \end{array} .$$

195

196 **Definition 2.9.** Let (z, u) be a singular extremal on $[0, T]$ of minimal order. The singular ex-
 197 tremal is called strict if the adjoint vector is unique up to a scalar (that is unique in PT^*M)
 198 on $[0, T]$. In the strict case, a singular trajectory $(x, u) = (\Pi_M(z), u)$ on $[0, T]$ is called

- 199 (1) *Abnormal* or exceptional if for every $t \in [0, T], H_X(z(t)) = 0$,

- 200 (2) *Hyperbolic* if for every $t \in [0, T]$, $H_X(z(t)) \{H_Y, H_X\}, H_Y(z(t)) > 0$,
 201 (3) *Elliptic* if for every $t \in [0, T]$, $H_X(z(t)) \{H_Y, H_X\}, H_Y(z(t)) < 0$.

202 According to the high order Maximum Principle [13], the hyperbolic trajectories are can-
 203 didates to time-minimal control, while elliptic trajectories are candidates to time-maximal
 204 control, while abnormal (exceptional) can be both.

205 2.3. The 2d–case

206 The 2d–case is a specific situation but can be used to illustrate the general result avoiding
 207 technical difficulties. Without losing any generality, one can take $M = \mathbb{R}^2$ and we denote
 208 by $x = (x_1, x_2)$ the coordinates while $p = (p_1, p_2)$ denotes the non zero adjoint vector. We
 209 introduce the following determinantal sets called respectively the *singular locus* \mathcal{S} and the
 210 *collinearity locus* \mathcal{C} :

$$\mathcal{S} : \{x, \det(Y, [Y, X])(x) = 0\}, \quad \mathcal{C} : \{x, \det(Y, X)(x) = 0\}.$$

211 One will assume that Y is not vanishing so that one can choose (local) coordinates with
 212 $Y = \frac{\partial}{\partial x_2}$. Moreover we assume that \mathcal{S} and \mathcal{C} are regular and intersect transversally at the
 213 point 0 . If $D := \det(Y, [[Y, X], Y])$ is not vanishing when restricted to \mathcal{S} , the singular control
 214 is given by the feedback: $u_s(x) = -\frac{D'(x)}{D(x)}|_{\mathcal{S}}$, where $D' := \det(Y, [[Y, X], X])$. Moreover using
 215 $H_Y = 0$, the adjoint vector is such that $p_2 = 0$ identically.

216 We choose coordinates preserving Y so that \mathcal{S} coincides with the x_1 –axis. In a neigh-
 217 bourhood of 0 , using the action of the feedback group, the system reads:

$$\begin{aligned} \dot{x}_1 &= \lambda x_1 - x_2^2 + o_{x_1}(x_2^2), \\ \dot{x}_2 &= u, \end{aligned} \tag{12}$$

218 where $o_{x_1}(x_2^2)$ represents a term of order ≥ 3 in the jets space of (X, Y) along the singu-
 219 lar line, identified to the x_1 –axis (the singular dynamics being feedback equivalent to the
 220 linear dynamics).

221 Assuming $\lambda \neq 0$ and restricting the dynamics to singular line identified to $x_2 = 0$,
 222 straightforward computation gives us that the singular dynamics is $\dot{x}_1 = \lambda x_1$ and is foliated
 223 by the abnormal points $x_1 = 0$, the hyperbolic arc in $x_1 > 0$ and the elliptic arc in $x_1 < 0$.

224 The adjoint dynamics using $p_2 = 0$ is defined by the adjoint system $\dot{p}_1 = -\lambda p_1 + o_{x_1}(x_2)$.
 225 Hence linearized adjoint dynamics reads: $\dot{p}_1 = -\lambda p_1$.

226 In particular, the abnormal singular point $x = 0$ lifts into a ray in the projective bundle
 227 defined by $p_2 = 0$ and $p_1(t) = e^{-\lambda t} p_1(0)$. The linearized Hamiltonian dynamics takes the
 228 form

$$\dot{x}_1 = \lambda x_1, \quad \dot{p}_1 = -\lambda p_1.$$

229 Clearly λ is a feedback invariant and using the projective coordinates $v = x_1 / p_1$, leads to
 230 the dynamics $\dot{v} = 2\lambda v$ so that 2λ is a *projectivized feedback invariant*.

231 From this analysis one deduces the following.

232 **Theorem 2.10.** *In the 2d–case there exist a nonempty open set of pairs (X, Y) for the Whit-*
 233 *ney topology such that:*

- 234 (1) *Equilibria of the singular dynamics are isolated and reduced to abnormal equilibria*
 235 *x_0 defining the singular lines in M with dynamics $\dot{x} = \lambda(x_0)x$.*
 236 (2) *Each such point defines a ray $z(t) = e^{-\lambda(x_0)t} z_0$, $z_0 \in \ell$ (ℓ being a line in $T_{x_0}^* M$).*
 237 (3) *The singular line is foliated into the abnormal equilibrium and hyperbolic, elliptic*
 238 *arcs.*
 239 (4) *The eigenvalue $2\lambda(x_0)$ is a projective feedback invariant.*

240 **Remark 1.** Introducing the clock one form: $\alpha = p dx$ outside the collinear set, the singular
 241 lines are the zero of $d\alpha = dp \wedge dx$.

242 2.4. The 3d-case

243 The previous planar case can be generalized to the three dimensional case, which is a very
 244 rich situation and can be treated similarly, paving the road to the general case.

245 Using (8), we introduce the determinantal mappings:

$$\begin{aligned} D &= \det(Y, [Y, X], [[Y, X], Y]), & D' &= \det(Y, [Y, X], [[Y, X], X]), \\ D'' &= \det(Y, [Y, X], X). \end{aligned} \quad (13)$$

246 Assume that D is non zero, one has the following proposition.

247 Proposition 2.11.

- 248 • *Singular trajectories of minimal order are solutions of the dynamics:*

$$\frac{dx}{dt}(t) = X_s(x) := X(x) + u_s(x) Y(x), \quad (14)$$

249 where the singular controls u_s is given by the feedback:

$$u_s(x) = -\frac{D'(x)}{D(x)}. \quad (15)$$

- 250 • *The sets $D'' = 0$, $DD'' > 0$ and $DD'' < 0$ are invariant for the singular dynamics and*
 251 *correspond respectively to abnormal, hyperbolic and elliptic trajectories.*
 252 • *The adjoint vector in the projective space $PT^*\mathbb{R}^3$ is uniquely defined by the relations*
 253 *$H_Y = \{H_Y, H_X\} = 0$.*

254 Introducing the clock form $\alpha = p dx$ defined by the relations: $H_X = 1$, $H_Y = \{H_Y, H_X\} = 0$,
 255 outside the abnormal locus $D'' = 0$, the singular trajectories are the characteristics of $d\alpha$.

256 Clearly we have:

257 **Lemma 2.12.** *The feedback group G_f acts on the singular dynamics by change of coordi-*
 258 *nates only.*

259 From which we deduce:

260 **Proposition 2.13.** *The singular points of (14) are abnormal equilibria and denoting by J*
 261 *the Jacobian matrix of (14) at such points then the whole spectrum $\sigma(J)$ is feedback inva-*
 262 *riant. Each equilibrium point x_0 defines a ray solution in the projective cotangent space*
 263 *given by $z(t) = e^{-\lambda t} z(0)$, where x_0 is the canonical projection of $z(0)$, $\lambda \in \sigma(J)$.*

264 **2.5. The general case $n \geq 3$**

265 In this case, more technicality is necessary, but the result follows mainly from the proof of
266 Lemma 1 in the reference [5].

267 One needs the following.

268 **2.5.1. Ad-condition and the bad set of infinite codimension**

269 Given a pair (X, Y) of vector fields denote by $\text{ad}X$ the operator defined by: $\text{ad}^0 X(Y) = Y$,
270 $\text{ad}X(Y) = [X, Y]$ and inductively: $\text{ad}^k X(Y) = [\text{ad}^{k-1} X \cdot Y, Y]$ for $k \geq 2$. Denote by $\text{ad}H_X$ the
271 induced operator on the Hamiltonians: $\text{ad}H_X \cdot H_Y = \{H_X, H_Y\}$.

272 **Definition 2.14.** For N large enough we define the following subset of $J^N TM \times J^N TM$:

- 273 (1) $B'_\ell(N)$ is the subset of all couples $(j_x^N X, j_x^N Y)$ such that:
274 $\dim \text{span} \{X(x), Y(x), [X, Y](x)\} \leq 1$.
275 (2) \hat{B}''_ℓ is the subset of $J^N TM \times J^N TM \times \mathbb{R}$ of all triples $(j_x^N X, j_x^N Y, a)$ such that:
276 (i) $Y(x) \neq 0$
277 (ii) $X(x) = aY(x)$
278 (iii) $\dim \text{span} \{ \text{ad}^k G_a(Y)(x), 0 \leq k \leq n-1, [[X, Y], Y](x) \} < n$, where $G_a = X - aY$.
279 (3) Denote by $B''_\ell(N)$ the canonical projection of $\hat{B}''_\ell(N)$ on $J^N TM \times J^N TM$. Let $B_\ell(N) =$
280 $B'_\ell \cup B''_\ell(N)$.

281 From the proof of Lemma 1 in [5], one has:

282 **Proposition 2.15.** Let (X, Y) be a pair in $VF(M) \times VF(M)$ such that for all $x \in M$,
283 $(j_x^N X, j_x^N Y) \notin B_\ell(N)$. Then:

- 284 (1) Let (z, u) be a singular extremal on $[0, T]$ such that $\dim \text{span} \{X(x(t)), Y(x(t))\} \leq 1$,
285 where x is the canonical projection of z . Then $x(\cdot)$ is constant and is an abnormal
286 singular arc reduced to a point x_0 .
287 (2) The extremal $z(\cdot)$ is of minimal order and strict and there exist a line $\ell \in T_{x_0}^* M$ so that
288 $z(t) = e^{-\lambda t} z_0$, $z_0 \in \ell$ and the control u is constant a.e. Hence $z(\cdot)$ is a ray solution.
289 (3) The point x_0 is a forced abnormal equilibrium contained in the collinear set and
290 let (A, b) be the linearized dynamics (7) at (x_0, u) , then (A, b) are constant and
291 $\text{span} \{b, Ab, \dots, A^{n-1}b\}$ is of codimension one. The line ℓ is orthogonal to this space.

292 **Theorem 2.16** (Main theorem for $n \geq 3$). There exist an open set of pairs (X, Y) for the C^∞ -
293 Whitney topology such that:

- 294 (1) Every singular extremal pair (z, u) on $[0, T]$ is with minimal order and strict.
295 (2) Every singular trajectory reduced to a point x_0 is abnormal and x_0 is a forced abnormal
296 equilibrium associated to a ray solution $z(t) = e^{-\lambda t} z(0)$, $z(0) \in \ell$, with ℓ a line in
297 $PT_{x_0}^* M$.
298 (3) Every abnormal equilibrium is isolated.
299 (4) The pair (A, b) is not controllable and $\text{span} \{b, Ab, \dots, A^{n-1}b\} = n-1$. The unique un-
300 controllable mode satisfies the dynamics $\dot{x} = \lambda x$.
301 (5) The whole spectrum of the linearized dynamics in $PT_{x_0}^* M$ is feedback invariant.

302 **Proof.** The proof follows from [5] and standard linear geometric control theory. More pre-
303 cisely, from linear theory, if the pair (A, b) is controllable, the pole placement theorem [23]

304 asserts that one can assign every spectrum using a linear gain control: $u = kx$. On the
 305 opposite, the non controllable modes cannot be modified. In the strict case, there exist a
 306 single uncontrollable mode. \square

307 2.5.2. Application to generic properties of pairs (X, Y, φ) .

308 Practically one aim of biological models is to describe equilibria and their stability prop-
 309 erty. From control point of view, one can choose Y in a given class and the Mayer cost to
 310 be maximized defines a family of terminal manifolds $N(d)$ of codimension one given as
 311 the level sets: $\{x, \varphi(x) = d\}$. Take a point $x \in N$, we denote by $n(x)$ the normal vector to
 312 N at x , and accessibility properties near the terminal point can be classified in a generic
 313 context for the C^∞ -Whitney topology on the triples: (X, Y, N) using the so-called transver-
 314 sality condition. This amounts to maximize the scalar product: $n \cdot \dot{x} = n \cdot (X + uY)$ for all u
 315 in a feasible interval, which can be taken as $[-1, +1]$.

316 This leads to stratify the final target $N(d)$ into:

- 317 • The switching locus $\Sigma : \{x \in N, n(x) \cdot Y(x) = 0\}$
- 318 • The singular locus $\mathcal{S} : \{x \in N, n(x) \cdot [Y, X](x) = 0\}$
- 319 • The exceptional locus $\mathcal{E} : \{x \in N, n(x) \cdot X(x) = 0\}$.

320 In particular this leads, for fixed pairs (X, Y) , to consider specific critical manifolds. In
 321 our study we consider manifolds N for which: $\Sigma \cap \mathcal{S} \cap \mathcal{E} \neq \emptyset$, to analyze

- 322 • time-minimal control syntheses,
- 323 • controlled stability.

324 This will be studied in the next sections using algebraic computations of equilibria on
 325 the Lotka-Volterra models.

326 3. Controlled Lotka-Volterra model

327 3.1. A brief recap about controlled Lotka-Volterra related to microbiote control

328 **Definition 3.1.** A controlled Lotka-Volterra dynamics is a control system of the form

$$\frac{dx}{dt}(t) = (\text{diag}x(t)) (Ax(t) + r + u(t)\mathcal{C}) \quad (16)$$

329 with $x := (x_1, \dots, x_n)^\top \in \mathbb{R}_{\geq 0}^n$, $A = (a_{ij})$, $r = (r_1, \dots, r_n)^\top$ and $\mathcal{C} = (\epsilon_1, \dots, \epsilon_n)^\top$ are constant vec-
 330 tors, $u(t)$ represents the control intensity, which can be taken in $[0, 1]$. The free dynamics
 331 is called *regular* if the matrix A is invertible. One can extend the dynamics to the whole \mathbb{R}^n
 332 and the control intensity to the whole \mathbb{R} .

333 An *interior equilibrium* is a point x in $\mathbb{R}_{> 0}^n$ such that $Ax + r = 0$ i.e. $x = A^{-1}r$. To each
 334 Lotka-Volterra dynamics one can assign in the regular case up to 2^n equilibria by consid-
 335 ering all the induced Lotka-Volterra models with extinction of at most one species x_i (i.e.
 336 $x_i = 0$). For the controlled Lotka-Volterra model, the infecting agent population is denoted
 337 x_1 , hence vermin reduction aims to minimize the x_1 -population.

338 **Lemma 3.2.** Consider the dynamics (16) and let $\Omega = (K_1, \dots, K_n)^\top$ be an interior equili-

339 *brium. Then there exist coordinates such that the dynamics (16) can be written:*

$$\dot{v}_i = -(v_i + 1) \left(\sum_{j=1}^n a_{ij}^* v_j + u \epsilon_i \right), \quad i = 1, \dots, n. \quad (17)$$

340

341 **Proof.** Let y_i be the dimensionless coordinates $y_i = x_i / K_i$, $i = 1, \dots, n$ so that the dynamics
342 (16) with $A \leftarrow -A$ written as $\dot{x}_i = x_i \left(r_i - \sum_{j=1}^n a_{ij} x_j + u \epsilon_i \right)$, $i = 1, \dots, n$, becomes

$$\dot{y}_i = y_i \left(r_i - \sum_{j=1}^n (a_{ij} K_j) y_j + u \epsilon_i \right), \quad i = 1, \dots, n. \quad (18)$$

343 Denote $A^* = (a_{ij}^*) = (K_i a_{ij})$. By construction, the interior equilibrium is normalized to
344 $\Omega = (1, \dots, 1)$ so that: $r_i = \sum_{j=1}^n a_{ij}^*$. Hence (18) becomes

$$\dot{y}_i = y_i \left(\sum_{j=1}^n a_{ij}^* (1 - y_j) + u \epsilon_i \right), \quad i = 1, \dots, n.$$

345 Therefore if we set $v_i = y_i - 1$ the dynamics takes the form

$$\dot{v}_i = -(v_i + 1) \left(\sum_{j=1}^n a_{ij}^* v_j - u \epsilon_i \right), \quad i = 1, \dots, n. \quad (19)$$

346 It can be written shortly as:

$$\dot{v} = -(\text{diag}(1 + v)) (A^* v - u \epsilon),$$

347 where the equilibrium is normalized to 0. □

348 Therefore this triggers to consider controlled Lotka–Volterra model of the form
349 $-(\text{diag}(v + 1)) (Av - u \epsilon)$ for which we have the following Lemma.

350 **Lemma 3.3.** *Consider the controlled Lotka–Volterra model $\dot{x} = -(\text{diag}(x + 1)) (Ax - u \epsilon)$
351 with interior equilibrium $x = 0$. Denote $X(x) = -(\text{diag}(x + 1))A$, $Y(x) = (\text{diag}(x +$
352 $1)) \epsilon$ so that $-A = \frac{\partial X}{\partial x}(0)$ and $Y(0) = \epsilon$. Hence $\text{span} \{ \text{ad}^k X \cdot Y(0), k = 0, \dots, n - 1 \} =$
353 $\text{span} \{ \epsilon, A \epsilon, \dots, A^{n-1} \epsilon \}$. Therefore $(x, u) = (0, 0)$ is an abnormal strict singular point if and
354 only if the rank of the Kalman matrix $K = [\epsilon, A \epsilon, \dots, A^{n-1} \epsilon]$ is strictly less than $n - 1$.*

355 **Corollary 3.4.** *The pair (A, b) is controllable if and only if ϵ is a cyclic vector of A .*

356 This leads to easily characterize every pair (A, ϵ) using a Jordan decomposition of A
357 such that $(0, 0)$ is an (abnormal) singular trajectory.

358 **Example 3.5.** Take a matrix A with Jordan blocks with equal eigenvalues e.g. the diagonal
359 matrix $A = \text{diag}(\lambda_1, \lambda_1, \lambda_2)$. Then for every vector ϵ the pair (A, ϵ) is not controllable.

360 **3.2. Some examples of case studies**

361 3.2.1. *The prey–predator model*

362 This historical model [21], using the (x, y) coordinates, takes the form

$$\frac{dx}{dt} = x(\lambda_1 + \mu_1 y) + u\epsilon_1 y, \quad \frac{dy}{dt} = y(\lambda_2 + \mu_2 x) + u\epsilon_2 y, \quad (20)$$

363 which covers both the elliptic and hyperbolic case.

364 The point $\Omega = (-\lambda_2/\mu_2, -\lambda_1/\mu_1) := (K_1, K_2)$ is the interior equilibrium in the quad-
 365 rant $x, y > 0$ provided that $\lambda_1\mu_1, \lambda_2\mu_2 < 0$. Introduce the dimensionless coordinates $x \leftarrow$
 366 $x/(-\lambda_2/\mu_2)$ and $y \leftarrow y(-\lambda_1/\mu_1)$ we obtain the system:

$$\dot{x} = \lambda_1 x(1 - y) + ux\epsilon_1, \quad \dot{y} = \lambda_2 y(1 - x) + ux\epsilon_2,$$

367 where the interior equilibrium is normalized to $\Omega = (1, 1)$.

368 The Jacobian matrix at Ω is

$$J = \begin{pmatrix} 0 & -\lambda_1 \\ -\lambda_2 & 0 \end{pmatrix}$$

369 and is elliptic if $\lambda_1\lambda_2 < 0$ and hyperbolic if $\lambda_1\lambda_2 > 0$.

370 The collinearity locus is $\mathcal{C} : xy[\epsilon_2\lambda_1(1 - y) - \epsilon_1\lambda_2(1 - x)] = 0$ and contains $\Omega = (1, 1)$ by
 371 construction.

372 The singular locus is $\mathcal{S} : xy[\epsilon_1^2\lambda_2x - \epsilon_2^2\lambda_1y] = 0$ and defines the interior line for $xy \neq 0$
 373 given by $y = \frac{\epsilon_1^2\lambda_2}{\epsilon_2^2\lambda_1}x$. Hence we have:

- 374 • *Elliptic case:* $\lambda_1\lambda_2 < 0$. The singular line is not contained in the cone $x, y > 0$.
- 375 • *Hyperbolic case:* $\lambda_1\lambda_2 > 0$. The singular line is contained in the cone of positive
 376 population $x, y > 0$.

377 The crucial point of the classification is to compute abnormal points, intersection of
 378 such two interior lines. At such point, the analysis of 3.2 applies.

379 A richer situation making interacting the elliptic and hyperbolic cases is to consider the
 380 model:

$$\frac{dx}{dt} = (1 - u)X(x) + uY(x), \quad u \in [0, 1],$$

381 with

$$X = \lambda_1 x(1 - y) \frac{\partial}{\partial x} + \lambda_2 y(1 - x) \frac{\partial}{\partial y}, \quad Y = x(\lambda'_1 + \mu'_1 y) \frac{\partial}{\partial x} + y(\lambda'_2 + \mu'_2 x) \frac{\partial}{\partial y},$$

382 which leads to the system: $\dot{x} = X + u(Y - X)$ connecting the elliptic case to the hyperbolic
 383 case. It is an extension of models (16). Straightforward computations lead to an interior
 384 collinearity locus, which is defined by a quadratic mapping vs. a linear map in the prey–
 385 predator model, while the interior singular locus is defined by a cubic mapping vs. a linear
 386 map. More generally automatic computations lead to analyze all the $2d$ –cases.

387 3.2.2. 3d–case studies

388 The 3d–case is a very complicated situation due to the complexity of the classification of
 389 the singular dynamics. This is not surprising in the context of dynamical systems due to
 390 the phenomenon of chaos. For Lotka–Volterra models the situation can be tamed if we
 391 consider the case of *competitive 3d*–models. Restricting to this case, we shall make a brief
 392 recap of this theory based on the presentation of [3] introducing the concept of carrying
 393 simplicia and the May–Leonard model [15] as a case study.

394 **Definition 3.6.** If the Lotka–Volterra dynamics takes the form: $\dot{x} = (\text{diag } x)(r - Ax)$, where
 395 $a_{ij}, r_i > 0$ for all $i, j = 1, \dots, n$ the system is called competitive.

396 **Property 3.7.** For a competitive Lotka–Volterra system, we have:

- 397 • The equilibrium $x_e = 0$ is an unstable node.
- 398 • Every positive trajectory in the $\mathbb{R}_{\geq 0}^n$ –space is bounded.

399 The interesting case, in the non trivial case, is when the dynamics admits an unique
 400 equilibrium in the cone $\mathbb{R}_{> 0}^n$. Without loss of generality, it can be taken as $\Omega = (1, \dots, 1)$
 401 using Lemma 3.2.

402 Denoting in short by $X(x)$ the vector field $(\text{diag } x)(r - Ax)$ and by φ_t be the (local) pa-
 403 rameter group $\{\exp tX\}$, one can assume that X is complete and let $\Lambda^+(x)$ denotes the
 404 ω –limit set of a point x . Recall that $p \in \Lambda^+(x)$ if there exist a sequence $t_k \rightarrow +\infty$ such that
 405 $\exp t_k X(x) \rightarrow p$ when $k \rightarrow +\infty$. One can take [18] as a reference for the properties of such
 406 set in relation with stability analysis.

407 **Definition 3.8.** Since every positive trajectory is bounded in $\mathbb{R}_{\geq 0}^n$ the basin of repulsion of
 408 the unstable node $x_e = 0$ is bounded and its boundary is called the *carrying simplex* and is
 409 denoted by Π .

410 The following result holds [11].

411 **Theorem 3.9.** In the competitive case, every positive trajectory of the dynamics in $\mathbb{R}_{\geq 0}^n \setminus \{0\}$ is
 412 asymptotic to one trajectory in Π and Π is a Lipschitz submanifold transverse to all strictly
 413 positive direction and homeomorphic to the probability simplex: $\Delta_1 : \sum_{i=1}^n x_i = 1$.

414 **Example 3.10.** In many cases, the carrying simplex can be computed and the dynamics
 415 on Π describes the asymptotic behaviours of positive trajectories. The simplest example
 416 where it differs from Δ_1 is given by the 2d–system:

$$\dot{x} = x(1 - x - y/2), \quad \dot{y} = y(1 - 3x - y).$$

417 The only equilibria are the origin and the non interior equilibria: $(1, 0)$ and $(0, 1)$. The car-
 418 rying simplex is the graph of the function $y(x) = (1 - x)^2$ on $[0, 1]$ and is a trajectory joining
 419 the saddle $(0, 1)$ to the attracting node $(1, 0)$.

420 Clearly the computation of this set leads to solve the global stability problem, see [24].
 421 This opens the road to the concept of *controlled stability* of a chosen point in Π using the
 422 controlled Lotka–Volterra model (see Section 4.2).

423 3.2.3. The May–Leonard model [15]

424 It is a basic model where the carrying simplex coincides for some parameters of the model
 425 with the probability simplex and where the dynamics can be investigated using *bifurcation*

426 *analysis*. We follow the presentation of [3], see also [2].

427 **Definition 3.11.** The *May–Leonard model* has the dynamics

$$\begin{aligned}\dot{x} &= x(1 - x - \alpha y - \beta z) \\ \dot{y} &= y(1 - \beta x - y - \alpha z) \\ \dot{z} &= z(1 - \alpha x - \beta y - z)\end{aligned}\tag{21}$$

428 and we denote by $A = \begin{pmatrix} 1 & \alpha & \beta \\ \beta & 1 & \alpha \\ \alpha & \beta & 1 \end{pmatrix}$ the associated (circular) matrix.

429 **Property 3.12.** For $\alpha, \beta > 0$ and $\alpha + \beta = 2$, the carrying simplex Π coincides with the proba-
430 bility simplex $x + y + z = 1$ and eliminating in (21) the z -variable leads to the dynamics on
431 Π :

$$\begin{aligned}\dot{x} &= \frac{\alpha - \beta}{2} x(1 - x - 2y) \\ \dot{y} &= -\frac{\alpha - \beta}{2} y(1 - 2x - y)\end{aligned}\tag{22}$$

432 with $\alpha + \beta = 2$. The system is conservative (i.e. with zero divergence) and we have a canonical
433 Hamiltonian system associated to

$$H(x, y) = \frac{\alpha - \beta}{2} (1 - x - y)xy$$

434 so that in the open triangle $\mathcal{T} : \{(x, y) > 0, x + y < 1\}$ all the solutions are periodic.

435 More generally for arbitrary parameters α, β the eigenvalues of A can be determined,
436 see [15] for a discussion.

437 The equilibria points are the origin, three single population of the form $(1, 0, 0)$ and three
438 two populations solutions of the form $(1 - \alpha, 1 - \beta, 0)/(1 - \alpha\beta)$. The interior equilibrium is
439 $\Omega = (1, 1, 1)/(1 + \alpha + \beta)$, where the linearized dynamics is determined by the eigenvalues of
440 A .

441 Therefore the model is a good case study to apply our analysis in particular taking the
442 control direction Y tangent to the $2d$ -plane. This allows to get a complete classification of
443 all cases with respect to the parameters (ϵ_1, ϵ_2) and computations associated to this exam-
444 ple are given in Section 4.2

445 4. Applications and numerical results

446 4.1. Discussion about the nonemptiness property of the good set in Theorem 2.16

447 4.1.1. Nonemptiness in the controlled Lotka–Volterra model

448 Using example 3.5 from Section 3.1, consider the controlled Lotka–Volterra model:
449 $-\text{diag}(x + 1) [Ax - u\mathbf{C}]$ in \mathbb{R}^3 with:

- 450 • $A = \text{diag}(\lambda_1, \lambda_1, \lambda_3)$,
- 451 • $\mathbf{C} = (\epsilon_1, \epsilon_2, \epsilon_3)^\top$, $\epsilon_1 \neq \epsilon_2$.

452 Hence since the matrix A contains two identical eigenvalues, one deduces that for every
 453 \mathcal{C} , the equilibrium point $x_e = 0$ is abnormal with $u_e = 0$ being the abnormal control.

454 The computation of the determinantal mappings D, D' defined in Section 2.4 yields the
 455 singular control $u_s(x) = -D'(x)/D(x) = \lambda_3(x_1 - x_2)/(\varepsilon_1 - \varepsilon_2)$. By construction at $x = 0$, one
 456 has $u_s(0) = u_e = 0$. Moreover the spectrum of the linearized singular dynamics at 0 is $\{\lambda_3 -$
 457 $\lambda_1, -\lambda_3, -\lambda_1\}$, proving that the singular point 0 is isolated and that the set introduced in
 458 Theorem 2.16 is nonempty.

459 The calculation can be generalized to the n -dimensional Lotka–Volterra case.

460 4.1.2. Emptyness in the quadratic case

461 **Proposition 4.1.** *Let (Q, b) be a pair of vector fields on \mathbb{R}^3 with Q being a quadratic homo-*
 462 *geneous and b being a constant vector. Then we have:*

- 463 (1) • $D = \det(b, [b, Q], [[b, Q], b])$: linear form
 464 • $D' = \det(b, [b, Q], [[b, Q], Q])$: cubic form
 465 • $D'' = \det(b, [b, Q], Q)$: cubic form.

466 Hence the singular dynamics

$$\frac{dx}{dt}(t) = Q(x(t)) - \frac{D'(x(t))}{D(x(t))}b$$

467 is homogeneous and quadratic.

- 468 (2) Let be the time reparameterization defined by $Dd\tau = dt$ so that the singular dynamics
 469 reads

$$\frac{dx}{d\tau}(\tau) = Q(x(\tau))D(x(\tau)) - D'(x(\tau))b$$

470 and is cubic. It can be projected on the projectivized space $P(\mathbb{R}^3)$. Moreover the map

$$\hat{\lambda}_s : (Q, b) \mapsto QD - D'b$$

471 is a semi-covariant.

472 **Definition 4.2.** Let $\dot{x} = H(x)$ be a differential equation on \mathbb{R}^n with H being a cubic ho-
 473 mogeneous vector field. A ray is a line ℓ so that the dynamics restricted to ℓ is given by
 474 $\dot{x}_1 = \lambda x_1^3$. In the generic case, $\lambda \neq 0$, it is an asymptotic direction but if $\lambda = 0$ it is a set of
 475 non isolated equilibria for the dynamics.

476 From which we deduce.

477 **Corollary 4.3.** *For every pair (Q, b) on \mathbb{R}^3 , every abnormal equilibrium point is not isolated*
 478 *so that in this family the set described in Theorem 2.16 is empty.*

479 Nevertheless, one can use for pair (Q, b) the projectivized singular dynamics on $P(\mathbb{R}^3)$ to
 480 compute feedback invariants. Indeed every ray projects onto an equilibrium point, where
 481 we can compute the linearized dynamics. We refer to [4] for the application of this result to
 482 classify the controlled Euler dynamics in the attitude control problem, where b describes
 483 the position of gas jet on the satellite.

484 **4.2. The May–Leonard model**

485 **4.2.1. Geometric properties**

486 Following Section 3.2.3, we study the asymptotic dynamics of the three dimensional May–
 487 Leonard model. This dynamics is characterized by the carrying simplex $\Pi : x + y + z = 1$.
 488 We then consider the restriction of (21) to the carrying simplex and the control directions
 489 are tangent to the carrying simplex. This procedure can be reproduced for general Lotka–
 490 Volterra systems, where we can select a set of species that satisfy a May and Leonard dyna-
 491 mics (see [8]). This leads to the system

$$\dot{\mathbf{x}} = X(\mathbf{x}) + u Y(\mathbf{x}), \quad \mathbf{x} = (x, y), \quad u \in [0, 1]$$

492 with

$$X = x(1 - x - 2y) \frac{\partial}{\partial x} - y(1 - 2x - y) \frac{\partial}{\partial y}, \quad Y = \epsilon_1 x \frac{\partial}{\partial x} + \epsilon_2 y \frac{\partial}{\partial y}. \quad (23)$$

493 The singular set and the collinearity locus are given respectively by

$$\mathcal{S} : \epsilon_2(\epsilon_1 + 2\epsilon_2)y + \epsilon_1(\epsilon_2 + 2\epsilon_1)x = 0 \quad \text{and} \quad \mathcal{C} : (\epsilon_1 + 2\epsilon_2)y + (\epsilon_2 + 2\epsilon_1)x = \epsilon_1 + \epsilon_2.$$

494 For $\epsilon_1 \neq \epsilon_2$, $\epsilon_1 \neq -2\epsilon_2$ and $\epsilon_2 \neq -2\epsilon_1$, their intersection $\mathcal{S} \cap \mathcal{C}$ is the point

$$x_{se} = \left(\frac{\epsilon_2}{\epsilon_2 + 2\epsilon_1}, \frac{\epsilon_1 + \epsilon_2}{\epsilon_2 - \epsilon_1} \right) = \left(\frac{\epsilon_1}{\epsilon_1 + 2\epsilon_2}, \frac{\epsilon_1 + \epsilon_2}{\epsilon_1 - \epsilon_2} \right) = \left(\frac{1}{1 + 2\kappa}, \frac{1 + \kappa}{1 - \kappa} \right), \quad \kappa = \frac{\epsilon_1}{\epsilon_2}$$

495 and the study of the components of x_{se} as functions of κ shows that x_{se} is in the positive
 496 orthant if $\kappa \in]-\infty, -2[\cup]-1/2, 0[$ and is outside the triangle $\mathcal{T} = \{\mathbf{x} = (x, y) > 0, x + y < 1\}$ for
 497 any value of κ (recall that in the triangle \mathcal{T} the free dynamics consists in periodic orbits).

498 For $x_e = (x_{1e}, x_{2e}) \in \mathcal{C}$, the value of the control $u_e(x_e)$ such that $X(x_e) + u_e Y(x_e) = 0$ is

$$u_e(x_e) = \frac{1 - 3x_{1e}}{\epsilon_1 + 2\epsilon_2}$$

499 and the spectrum of the Jacobian matrix $J(x_e) := \frac{\partial}{\partial \mathbf{x}} (X(\mathbf{x}) + u Y(\mathbf{x}))|_{\mathbf{x}=x_e}$ is

$$\sigma(J(x_e)) = \left\{ 3u(\epsilon_1 + \epsilon_2) \pm \frac{1}{2\sqrt{3}} \sqrt{11u^2(\epsilon_1 + \epsilon_2)^2 + 4(\epsilon_1 u + 1)(\epsilon_2 u - 1)} \right\}.$$

500 In particular,

- 501 • at $u = 0$, $\sigma(J(x_e)) = \left\{ \pm \frac{i}{\sqrt{3}} \right\}$,
- 502 • at $u = 1$, $\sigma(J(x_e)) = \left\{ 3(\epsilon_1 + \epsilon_2) \pm \frac{1}{2\sqrt{3}} \sqrt{11(\epsilon_1 + \epsilon_2)^2 + 4(\epsilon_1 + 1)(\epsilon_2 - 1)} \right\}$,
- 503 • at $u = u_e(x_{se})$, $\sigma(J(x_e)) = \left\{ \frac{\epsilon_1 + \epsilon_2}{\epsilon_1 - \epsilon_2}, -\frac{\epsilon_1 + \epsilon_2}{\epsilon_1 - \epsilon_2} \frac{3\epsilon_1 \epsilon_2}{(2\epsilon_1 + \epsilon_2)(2\epsilon_2 + \epsilon_1)} \right\}$. Note that in this case, the first
 504 eigenvalue corresponds to the noncontrollable mode of the system, while the second
 505 eigenvalue is not meaningful since it can be replaced by any value via pole shifting.

506 The singular dynamics $\dot{z} = \vec{H}_s(z)$ (restricted to Σ) has eigenvalues at $x = x_{se}$:

$$\left\{ -\frac{\epsilon_1 + \epsilon_2}{\epsilon_1 - \epsilon_2}, \frac{\epsilon_1 + \epsilon_2}{\epsilon_1 - \epsilon_2} \right\}$$

507 and $\lambda = \frac{\epsilon_1 + \epsilon_2}{\epsilon_1 - \epsilon_2}$ is a feedback invariant of the control system.

508 4.2.2. Direct and semi-direct methods

509 We present two numerical schemes to solve the time-minimal control problem for the
510 Lotka–Volterra class of models specifically a direct method and a semi-direct method.

511 The objective is to reach, from an initial position x_0 a terminal manifold of codimen-
512 sion one in minimum time, namely, this target is taken as a disk $N(\mathbf{x}) \leq 0$ centered on the
513 collinearity locus \mathcal{C} in which local controllability is guaranteed provided that the forcing
514 feedback is interior. This is an example of controlled stability.

515 There is no use comparing these methods in terms of computational time. The direct
516 method computes open-loop controls, while the semi-direct method computes closed-
517 loop controls, which can be used for real-time application since the trajectory is computed
518 step by step. In this sense we use the direct method to have an upper bound of the value
519 function and it is compared to the objective value associated to the semi-direct method
520 presented below.

521 Both methods are implemented in the WOLFRAM LANGUAGE using the Brent’s principal
522 axis method of the Mathematica’s routine FindMinimum.

523 **Direct method.** We consider the time-optimal control problem:

$$(OCP) \quad \min_{u(\cdot), T} \quad T$$
$$\begin{aligned} \dot{\mathbf{x}}(t) &= X(\mathbf{x}(t)) + u(t) Y(\mathbf{x}(t)), \quad u(t) \in [0, 1], \quad a.e. \quad t \in [0, T] \\ \mathbf{x}(0) &= x_0 \quad (\text{given}) \\ N(\mathbf{x}(T)) &\leq 0 \end{aligned}$$

524 where $\mathbf{x} = (x, y)$ and X, Y are given by (23).

525 We perform a discretization over the state and the control spaces for (OCP) to obtain
526 a nonlinear finite dimensional optimization problem. The optimization variables are the
527 values of the control at each time step and a primal-dual interior point method is used
528 to solve numerically the optimization problem. The optimality conditions – written as a
529 relaxation of the Karush–Kuhn–Tucker conditions – are determined using automatic dif-
530 ferentiation.

531 It is usually a quite robust method with respect to the initialization compared to indi-
532 rect methods based on the Pontryagin Maximum Principle. However it does not exploit the
533 geometric structure of the optimal control. The BOCOP software² provides an implemen-
534 tation of this method based on the IPOPT optimization solver³.

535 **Model predictive control method.** The semi-direct method is based on a sampled-data
536 control formulation of the problem, which is adapted to medical protocols that can be
537 used to cure the C. difficile infection. The optimal path is constructed iteratively, where at
538 each iteration we solve an optimal control problem on a reduced time horizon, whereas
539 the direct method discretizes the problem on the whole time interval.

540 In this sense, our method is closely related to model predictive control (MPC) widely
541 used for control theory applications [17, 22]. The current state of the method x_c is initial-

²www.bocop.org

³www.coin-or.github.io/Ipopt

542 ized to x_0 and is updated iteratively by solving the optimal control problems of the form

$$(OCP') \quad \min_{u \in \mathbb{R}^h} N(\mathbf{x}(t_h; u, x_c))$$

$$\dot{\mathbf{x}}(t) = X(\mathbf{x}(t)) + u_i Y(\mathbf{x}(t)), \quad u_i \in [0, 1], \quad a.e. \quad t \in [t_i, t_{i+1}], \quad i = 0, \dots, h-1,$$

$$\mathbf{x}(0) = x_c$$

543 where the integer h is the horizon, $0 = t_0 < \dots < t_h$ are given fixed times and $\mathbf{x}(\cdot; u, x_c)$
 544 is the state response associated to (u_1, \dots, u_h) and starting at x_c at $t = 0$. The algorithm
 545 terminates when $|N(x_c)|$ is smaller than a given threshold.

546 To solve (OCP') numerically, we derive a finite dimensional optimization problem by
 547 constructing an approximation of the objective function $u = (u_0, \dots, u_{h-1}) \mapsto N(\mathbf{x}(t_h))$ via
 548 an approximation of $\mathbf{x}(t_h; u, x_c)$ by discretizing the differential constraint with a midpoint
 549 rule (the discretization of the state on $[0, t_h]$ is finer than the partition $0 < t_1 < \dots < t_h$). The
 550 approximation of $N(\mathbf{x}(t_h; u, x_c))$ – together with its derivatives with respect to u_i , $i = 1, \dots, h$
 551 – can be computed offline using symbolic computations. Then we solve the optimization
 552 problem associated to (OCP') using a primal-dual interior point method. Once (OCP')
 553 is solved for the current value of x_c , we retrieve the values of t_1 and u_1 to update $x_c \leftarrow$
 554 $\mathbf{x}(t_1; u_1, x_c)$ and we iterate considering the resulting new instance of (OCP') .

555 4.2.3. Numerical results

556 We apply the previous numerical methods to the specific May–Leonard model and our aim
 557 is to control the system in the carrying simplex Π .

558 From the computations in Section 4.2.1, we can choose ϵ_1, ϵ_2 to fix the positions of x_{se}
 559 and x_e (corresponding to $u_e = 1$) and so that the singular dynamics goes toward \mathcal{C} and
 560 is hyperbolic. The target is taken as the circle N centered on \mathcal{C} and is reachable with an
 561 admissible control $u \in]0, 1[$.

562 We fix the initial point to $x_0 = (0.1, 0.8)$. The direct method converges in about 200 itera-
 563 tions to a bang–bang–singular–bang control (see Fig. 1) and the corresponding trajectory
 564 reaches N in less than 7.7 unit of time.

565 The semi-direct method is tuned with an horizon of $t_h = 2$ unit of time with $h = 3$ i.e. we
 566 compute three controls u_1, u_2, u_3 over this horizon. The resulting control seems to have the
 567 same structure as the control of the direct method. The trajectory reaches N in about 12
 568 unit of time (see Fig. 1). The depicted singular behavior depends on the size of the horizon
 569 t_h and the number of controls on that horizon. A smaller horizon t_h would typically keep
 570 the trajectory away from the singular arc.

571 5. Conclusion

572 In this article we describe feedback invariants to classify single–input control affine sys-
 573 tems in relation with the time–minimal control problem. They can be explicitly calculated
 574 using algebraic computations in the jets spaces of the dynamics at a given point corre-
 575 sponding to an abnormal stationary geodesic. They correspond at such points to the spec-
 576 trum of the projectivized Hamiltonian geodesic dynamics.

577 This result completes the computation of the feedback invariants related to the concept
 578 of conjugate points for both normal and abnormal geodesics. This gives a neat common
 579 geometric frame since those are related to the spectrum of the "projectivized" second-
 580 order intrinsic derivative, in relation with algebraic computations in the jets space of
 581 geodesics.

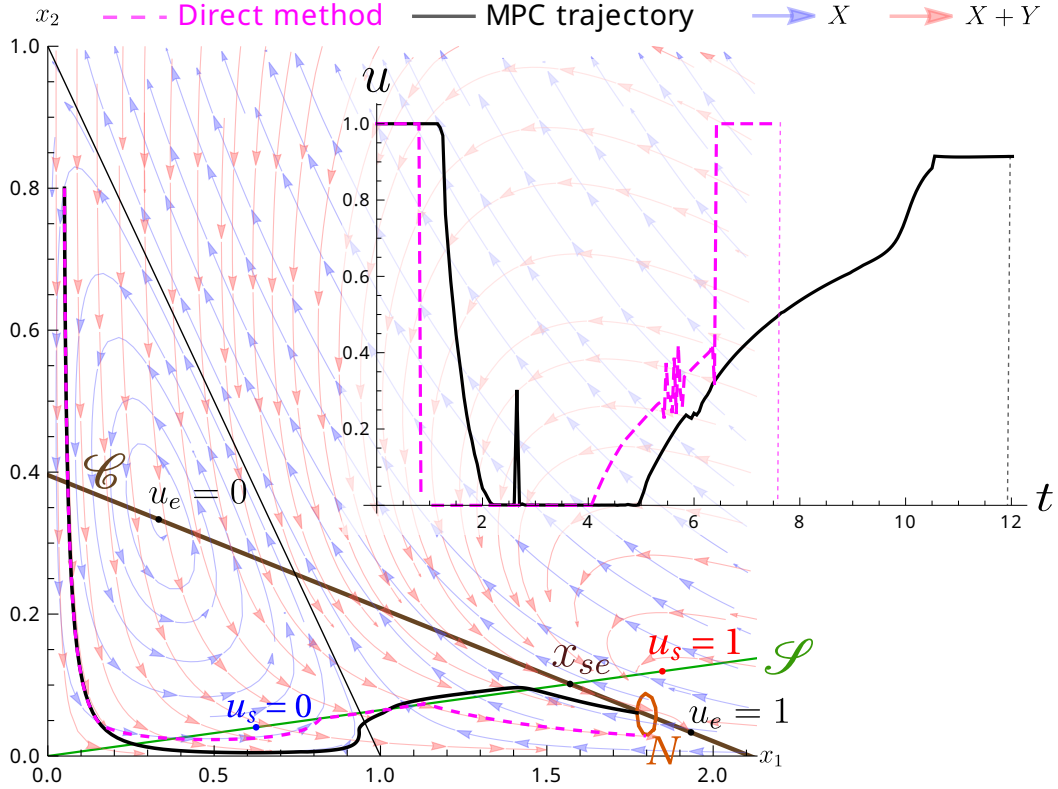


Figure 1. Numerical simulation performed on the May–Leonard model (21) with $\alpha = \beta = 2$, $\varepsilon_1 = 1$, $\varepsilon_2 = -2.9$. The aim is to reach in minimum time the ball of radius $\sqrt{0.03}$ centered at $x_C = (1.8, 0.058)$ located on the collinearity locus. (left) The dashed trajectory starting from $x_0 = (0.1, 0.8)$ and obtained with a direct method is bang–bang–singular–bang. It reaches the terminal circle N in less than 7.7 unit of time. The continuous MPC trajectory, obtained with an horizon of $t_h = 2$ and with three controls ($h = 3$), seems to reproduce the singular behavior. It reaches N in about 12 unit of time. (right) Time evolution of the control for the direct and MPC methods.

582 Our result is briefly applied to the controlled Lotka–Volterra, where abnormal stationary
583 geodesics are shifted equilibria of the free dynamics, which can be determined using lin-
584 ear calculations only. This gives an algebraic frame in relation with population dynamics
585 control. Another applications are for quadratic systems in relation for instance with the
586 attitude control problem of a rigid spacecraft.

587 A final numerical application shows the relation of the study to the time–minimal con-
588 trol problem, combining Pontryagin Maximum Principle with direct and semi–direct nu-
589 merical frame. Additionally it provides an example of controlled stability method popular
590 in biological models. More generally our analysis leads to structurally stable results based
591 on Lie algebraic computations in the jets space of the geodesics dynamics. It opens the
592 road to fine applications translating for instance results for the free dynamics of the May–
593 Leonard model [2] to controlled stability [9] or time optimal results, in the controlled case.

594 Preliminary results in this direction are obtained in [6, 8] to control the infection of a
595 complex microbiote with three species using probiotic and antibiotic treatment. The anal-
596 ysis of section 4.2 leads to analyze the effect of the therapy in the final phase of the treat-
597 ment (see [7]). Additional applications concern the controlled Euler equation where the
598 classification of the singular dynamics initialized in [4] is crucial in the attitude control
599 problem.

600 **Funding**

601 This work benefited from the support of the program PEPS "Jeunes chercheurs et jeunes
602 chercheuses" of Insmi 2022.

603 **References**

- 604 [1] A. AGRACHEV, I. ZELENKO, *On feedback classification of control-affine systems with*
605 *one and two-dimensional inputs*. SIAM J. Control Optim., **46**, no.4 (2007), pp.1431–
606 1460.
- 607 [2] S. BAIGENT, *Geometry of carrying simplices of 3-species competitive Lotka–Volterra*
608 *systems*. Nonlinearity, **26**, no.4 (2013), pp.1001–1029.
- 609 [3] S. BAIGENT, *Lotka–Volterra Dynamical Systems*. In: S. Bullett, T. Fearn, F. Smith, eds.
610 *Dynamical and Complex Systems*, LTCC Advanced Mathematics Series: Chapter **5**.
611 Singapore: World Scientific, 2017, 227 pages.
- 612 [4] B. BONNARD, *Feedback equivalence for nonlinear systems and the time optimal control*
613 *problem*. SIAM J. on Control and Optim., **29** (1991), pp. 1300–1321.
- 614 [5] B. BONNARD, I. KUPKA, *Generic properties of singular trajectories*. Ann. Inst. H.
615 Poincaré Anal. Non Linéaire, **14**, no.2 (1997), pp. 167–186.
- 616 [6] B. BONNARD, J. ROUOT, *Optimal Control of the Controlled Lotka–Volterra Equations*
617 *with Applications - The Permanent Case*. SIAM J. Appl. Dyn., **22**, no. 2 (2023), pp.
618 2761–2791.
- 619 [7] B. BONNARD, J. ROUOT, *Optimal Control of the Lotka–Volterra Equations with Appli-*
620 *cations*. Ivan Kupka’s legacy. A tour through controlled dynamics, in AIMS Applied
621 math. **12** (2024), pp. 15–33.
- 622 [8] B. BONNARD, J. ROUOT, C. J. SILVA, *Geometric optimal control of the generalized Lotka–*
623 *Volterra model of the intestinal microbiome*. Optimal Control Applications and Meth-
624 ods, **45**, no. 2 (2024), pp. 544–574.
- 625 [9] F.H. CLARKE, Yu. S. LEDYAEV, L. RIFFORD, R.J. STERN, *Feedback stabilization and Lya-*
626 *punov functions*. SIAM J. Control Optim., **39**, no.1 (2000), pp.25–48.
- 627 [10] J.A. DIEUDONNÉ, J.B. CARRELL, *Invariant Theory, Old and New*. Academic Press, New
628 York, 1971, 85 pages.
- 629 [11] M.W. HIRSCH, *Systems of differential equations which are competitive or cooperative:*
630 *III. Competing species*. Nonlinearity, **1**, (1988), pp.51–71.
- 631 [12] E.W. JONES, P.S. CLARCKE, J.M. CARSLON, *Navigation of outcome in a generalized*
632 *Lotka–Volterra model of the microbiome*. Advances in Nonlinear Biological Systems,
633 Modeling and Optimal Control, AIMS on applied Maths **11** (2021), pp. 97–117.
- 634 [13] A.J. KRENER, *The high order maximal principle and its application to singular ex-*
635 *tremals*. SIAM J. Control Optim. **15** no. 2, (1977) pp. 256–293.
- 636 [14] J. MARTINET, *Singularities of smooth functions and maps*. London Mathematical
637 Society Lecture Note Series, **58**. Cambridge University Press, Cambridge-New York,
638 1982, 256 pages.
- 639 [15] R.M. MAY, W.J. LEONARD, *Nonlinear aspects of competition between three species*.
640 SIAM J. Appl. Math., **29** (1975), pp. 243–253.
- 641 [16] L.S. PONTRYAGIN, V.G. BOLTYANSKII, R.V. GAMKRELIDZE, E.F. MISHCHENKO, *The math-*
642 *ematical theory of optimal processes*. Oxford, Pergamon Press, 1964, 362 pages.
- 643 [17] J. B. RAWLINGS, D. Q. MAYNE, M. M. DIEHL, *Model Predictive Control: Theory, Com-*
644 *putation, and Design*. Nob Hill Publishing, LLC, 2020, 770 pages.

- 645 [18] N. ROUCHE, J. MAWHIN, *Equations Différentielles Ordinaires*. Masson, Paris, **2** (1973),
646 266 pages.
- 647 [19] S. SMALE, *On the differential equations of species in competition*. Journal of Mathe-
648 matical Biology, **3** (1976), pp. 5–7.
- 649 [20] R.R. STEIN, V. BUCCI, N.C. TOUSSAINT, C.G. BUFFIE, G. RÄTSCH, E.G. PAMER, et al.,
650 *Ecological modelling from time-series inference: insight into dynamics and stability of*
651 *intestinal microbiota*. PLoS Comp. Biology, **9** no. 12 (2013).
- 652 [21] V. VOLTERRA, *Leçons sur la théorie mathématique de la lutte pour la vie*. Les Grands
653 Classiques Gauthier-Villars. Éditions Jacques Gabay, Sceaux, 1990, 215 pages.
- 654 [22] Y. WANG, S. BOYD, *Fast model predictive control using online optimization*, IEEE
655 Transactions on control systems technology, **18** no. 2, (2010), 267–278.
- 656 [23] W.M. WONHAM, *Linear Multivariable Control*. Springer-Verlag, New York, 1985, 348
657 pages.
- 658 [24] E.C. ZEEMAN, M.L. ZEEMAN, *From local to global behavior in competitive Lotka-*
659 *Volterra systems*. Trans. Amer. Math. Soc., 355 (2003), pp. 713–734.